Available online at www.sciencedirect.com
ScienceDirect
Biochemical and Biophysical Research Communications 349 (2006) 145–153
BBRC
www.elsevier.com/locate/ybbrc

Intracellular accumulation of a 46 kDa species of mouse prion protein as a result of loss of glycosylation in cultured mammalian cells ☆

Subhabrata Biswas [a,1], Jan P.M. Langeveld [b], Donald Tipper [c], Shan Lu [a,*]

[a] *Laboratory of Nucleic Acid Vaccines, Department of Medicine, University of Massachusetts Medical School, 364 Plantation St., Worcester, MA 01605, USA*

[b] *Central Institute for Animal Disease Control Lelystad, Edelhertweg 15, 8219 PH Lelystad, The Netherlands*

[c] *Department of Molecular Genetics and Microbiology, 55 Lake Ave. North, University of Massachusetts Medical School, Worcester, MA 01655, USA*

Received 28 July 2006
Available online 14 August 2006

Abstract

Prion diseases are fatal neurodegenerative disorders characterized by the accumulation of an abnormal isoform (PrP^{Sc}) of the normal cellular prion protein (PrP^{C}) in the brain. Reportedly, abnormal N-linked glycosylation patterns in PrP^{C} are associated with disease susceptibility; thus, we compared the glycosylation status of normal and several mutant forms of the murine prion protein (MuPrP) in cultured mammalian cells. Substitution of the N-terminal signal sequence of normal MuPrP with a heterologous signal peptide did not alter glycosylation. When expressed without the C-terminal glycophosphatidylinositol anchor signal, the majority of MuPrP remained intracellular and unglycosylated, and a 46 kDa species (p46) of the unglycosylated PrP^{C} was detected on reducing gels. p46 was also observed when wild-type MuPrP was expressed in the presence of tunicamycin or enzymatically deglycosylated *in vitro*. A rabbit polyclonal antiserum raised against dimeric MuPrP cross-reacted with p46 and localized the signal within the Golgi apparatus. We propose that the 46 kDa signal is a dimeric form of MuPrP and in the light of recent studies, it can be argued that a relatively stable, non-glycosylated, cytoplasmic PrP^{C} dimer, produced as a result of compromised glycosylation is an intermediate in initiating conversion of PrP^{C} to PrP^{Sc} in sporadic transmissible spongiform encephalopathies.

Keywords: Prion; Dimerization; Glycosylation

Prions are believed to be responsible for a number of previously known but little-understood diseases classified under transmissible spongiform encephalopathies (TSEs), including kuru, Creutzfeldt–Jakob disease (CJD), fatal familial insomnia (FFI), and Gerstmann–Sträussler–Scheinker syndrome (GSS) in humans, scrapie in sheep, chronic wasting disease in cervids and bovine spongiform encephalopathy in cattle that is better known as mad cow disease [1]. According to the now widely accepted protein-only-hypothesis [2], the central event in the development of a prion disease is the conversion of PrP^{C} to PrP^{Sc}, an oligomerized misfolded form with the unusual property of acting as an autocatalytic promoter of its own conversion. As a consequence, the PrP^{Sc} oligomer is the infectious agent responsible for the TSE phenotype, and spontaneous production of the PrP^{Sc} oligomer in a normal neuron presumably leads to sporadic disease as the infection spreads. The detailed mechanism of this conversion, however, remains unclear. Since the conversion of PrP^{C} to the abnormal isoform may be a co- or post-translational event [3], analysis of the post-translational trafficking pathway of PrP^{C} is of paramount importance in elucidating the process of conversion to PrP^{Sc} under disease conditions.

☆ *Abbreviations:* PrP^{C}, prion protein cellular; PrP^{Sc}, prion protein scrapie; GPI, glycophosphatidylionositol; tPA, tissue plasminogen activator; MAb, monoclonal antibody; FITC, fluorescein isothiocyanate.

* Corresponding author. Fax: +1 508 856 6751.
E-mail address: shan.lu@umassmed.edu (S. Lu).
[1] Present address: Channing Laboratory, Department of Medicine, Brigham and Women's Hospital, Harvard Medical School, 221 Longwood Avenue, Boston, MA 02115, USA.

0006-291X/$ - see front matter © 2006 Elsevier Inc. All rights reserved.
doi:10.1016/j.bbrc.2006.08.035

Considerable amount of data indicate that the N-linked glycosylation status of PrP^C maybe a determinant of prion disease susceptibility [4]. Mutants of PrP^C whose glycosylation sites have been inactivated were found to accumulate intracellularly in cultured cells [5] and to acquire PrP^{Sc} like properties, including detergent insolubility and partial protease resistance [6]. These characteristics were also observed when wild-type PrP^C was expressed in cultured cells treated with tunicamycin, a specific inhibitor of N-linked glycosylation. Expression of PrP^C in which either or both of the N-linked glycosylation sites were inactivated in transgenic mice resulted in low level expression, altered intracellular trafficking and increased susceptibility to infection with a particular PrP^{Sc} strain [7]. More direct evidence for a role of unglycosylated PrP^C in pathogenesis is provided by the T183A mutation which results in loss of glycosylation and familial human prion disease [8,9].

Mature PrP^C is a sialoglycoprotein of 209 amino acids, normally attached to the cell surface via its glycophosphatidylinositol (GPI) anchor [10]. An N-terminal signal sequence of 22 amino acids directs the nascent polypeptide chain to the endoplasmic reticulum for further processing which includes cleavage of the signal sequence, addition of N-linked oligosaccharide chains at Asn181 and Asn197 (in human PrP; in mouse PrP the glycosylation sites are at Asn180 and Asn196), formation of a single disulphide bond in the C-terminal domain and cleavage of a C-terminal signal sequence directing attachment of the GPI moiety. Subsequently, the processed PrP^C is transported through the Golgi complex, where modification of the N-linked glycans to complex sugars occurs, and is finally transported to the outer surface of the plasma membrane, where it remains attached by its GPI anchor [11]. PrP^C constitutively cycles between the plasma membrane and intracellular membrane bound compartments [12] and shedding of PrP^C into the extracellular medium of neuronal SH-SY5Y cells has been observed, probably resulting from secretase like proteolytic cleavage of the protein and phospholipase mediated cleavage of the GPI moiety [13]. A soluble form of PrP^C that lacks the GPI moiety has been detected in serum [14,15]. In primary cultures of splenocytes and cerebellar granule cells, a substantial amount of PrP^C devoid of the GPI anchor is shed [16]. A small portion of endocytosed PrP^C undergoes endoproteolytic cleavage between residues 110–111 [17]. The role, if any, of the proteolytically cleaved PrP^C fragments in pathogenesis is not clear at this point.

We have investigated the effect of substitution of the wild-type N-terminal signal sequence and deletion of the C-terminal hydrophobic GPI anchor attachment signal and the central putative transmembrane domain (TM) on the glycosylation status of the normal mouse prion protein (MuPrP) in two cell lines, a neuronal and non-neuronal cell line using three different antibodies against MuPrP. Lack of the C-terminal GPI anchor attachment signal resulted in perturbation of the N-linked glycosylation of MuPrP that confirmed earlier data. We report for the first time an intracellular accumulation of ~46 kDa (p46) species induced by loss of wild-type N-linked glycosylation. The ~46 kDa signal consistently appeared upon enzymatic deglycosylation of MuPrP and during *in vitro* synthesis of MuPrP in the presence of an N-linked glycosylation inhibitor. This previously unreported species of the prion protein, given its molecular weight and reactivity with a rabbit polyclonal antibody raised against a dimeric MuPrP, is most likely a dimer of the normal MuPrP.

Materials and methods

DNA plasmid constructs expressing different MuPrPs. DNA encoding the full-length MuPrP cDNA, kindly provided by Dr. D.A. Harris, Washington University, St. Louis, MO, was used as a template for PCR amplification of the sequences of MuPrP described below. Each individual MuPrP inserts as shown in Fig. 1 was subcloned into the eukaryotic expression vector pJW4303 [18] which drives high level expression of the encoded gene from the CMV promoter. This variant of the MuPrP gene contains two Methionine residues at positions 108 and 111 defining the hamster 3F4 epitope, allowing specific detection of the transgenic species in the presence of endogenous murine PrP^C, which does not react [19]. This full-length "wild-type" MuPrP (amino acid residues 1–254), designated as wt-PrP, was amplified with the forward primer 5′-AGT CAC AAG CTT ATG GCG AAC CTT GGC TAC-3′ and reverse primer 5′-AGT CAC GGA TCC TAA ATC CCA CGA TCA GGA AGA TG-3′, digested with *Hin*dIII and *Bam*HI and inserted into similarly digested pJW4303. MuPrP (residues 23–254) was amplified with the primer set 5′-AGT CAC GCT AGC GGC CCT CTT TGTGAC TAT G-3′ and 5′-AGT CAC GGA TCC TAA ATC CCA CGA TCA GGA AGA TG-3′ and inserted as a *Nhe*I/*Bam*HI fragment downstream of the tPA leader sequence of pJW4303 vector and in frame with the MuPrP fragment. The

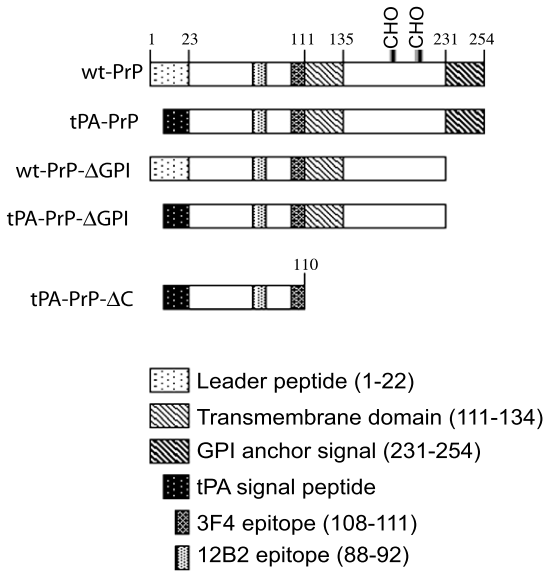

Fig. 1. Schematic representation of the different MuPrP encoding plasmid DNA constructs used in this study. Inserts encoding these constructs were cloned into eukaryotic expression vector pJW4303 under the control of CMV IE promoter/intron A. The position of the epitopes interacting with the two monoclonal antibodies 3F4 and 12B2 employed in this study is indicated. The numbers on the top correspond to the amino acid residues in the mouse prion protein and CHO denotes the N-linked glycosylation sites at residues 180 and 196. Numbers in parentheses correspond to the amino acid residues in MuPrP spanning the indicated domains.

DNA construct was designated as tPA-PrP. Both wt-PrP-ΔGPI (residues 1–230) and tPA-PrP-ΔGPI (residues 23–230) were amplified using the same forward primers as for wt-PrP and tPA-PrP and 5′-AGT CAC GGA TCC TAA TGG ATC TTC TCC CGT CGT AAT AGG-3′ as the common reverse primer and subcloned as a *Hin*dIII/*Bam*HI and *Nhe*I/*Bam*HI fragments, respectively. A sequence similar to the endoproteolytic cleavage product [17] was constructed by amplifying the N-terminal region corresponding to the amino acid residues 23–110 with the primers 5′-AGT CAC GCT AGC GGC CCT CTT TGTGAC TAT G-3′ and 5′-AGT CAC GGA TCC TAA ATG CTT CAT GTT GGT TTT TGG-3′ and subcloned as a *Nhe*I/*Bam*HI fragment in frame with the upstream tPA signal sequence of pJW4303 and designated as tPA-PrP-ΔC.

Antibodies. Mouse monoclonal antibody 12B2 was recently developed at CIDC-Lelystad from PrP^C-knockout mice [20] by immunizing with a synthetic peptide covering the domain corresponding to 97–115 of bovine PrP (85–103 of MuPrP) which was conjugated to KLH as previously described [21]. To detect the linear epitope specificities of the antibodies used, Pepscan analysis of solid-phase bound synthetic peptides was performed in an enzyme-linked immunosorbent assay-like setup as described previously [22,23]. To this end, a complete set of overlapping 15-mer peptides which covered complete amino acid sequence of bovine PrP were synthesized (GenBank Accession No. X55882). The specificity of 12B2 appeared to be: WGQGG, a sequence which is conserved in PrP^C of all species involved in this study. 3F4 mouse MAb directed against the residues 108–111 in our MuPrP constructs was a kind gift from Dr. Vishwanath Lingappa, University of California, San Francisco [19]. A7 is a rabbit polyclonal antibody raised against a dimeric form of MuPrP [24] provided by Dr. H.M. Schatzl, Technical University of Munich, Munich, Germany. MAb to the Golgi apparatus marker giantin [25] was a gift from Dr. H.P. Hauri, University of Basel, Switzerland.

Cell lines. Human embryonic kidney epithelial cells (293T), a non-neuronal cell line with a very low level of endogenous PrP^C expression [26], was used for *in vitro* transfection studies together with the mouse neuroblastoma, N2a (ATCC, number CCL-131) neuronal cell line. The cells were maintained in Dulbecco's modified Eagle's medium (Invitrogen, Carlsbad, CA) supplemented with 10% (v/v) fetal calf serum at 37 °C in a humidified atmosphere containing 5% CO_2.

In vitro expression of MuPrP DNA constructs. Human 293T and murine N2a cells were transiently transfected with the different MuPrP encoding plasmid DNA constructs described above and analyzed for *in vitro* expression. Transfection was done at approximately 50% cell-confluency in 60-mm dishes by calcium phosphate co-precipitation, using 10 μg of plasmid DNA per dish [27]. Transfection was also done with the pJW4303 vector without any inserts to serve as the negative control. To inhibit N-linked glycosylation of the exogenous MuPrP proteins, 5 μg/ml tunicamycin was added after transfection [6]. The supernatants and cell-lysate were harvested 72 h after transfection. The cell culture medium was centrifuged briefly to remove any cells and stored as the supernatant sample. The cell pellet was resuspended in an NP40 cell lysis buffer (50 mM Tris–Cl, pH 8, 150 mM NaCl, 1% NP40, and 1 mM PMSF), briefly sonicated and then incubated on ice for 30 min. Samples were then centrifuged at 3000*g* for 20 min at 4 °C and the supernatant was collected as the lysate sample. Protease sensitivity was assayed by incubating the samples at 4 °C for 60 min with Proteinase K (PK) at a concentration of 100 μg/ml in a total volume of 50 μl [28]. Prior to loading on SDS–PAGE, PK was inactivated by phenylmethylsulfonyl fluoride for 5 min.

Western blotting and deglycosylation. The MuPrP proteins expressed in 293T- and N2a-cell supernatants (20 μl total volume) and cell lysates (5 μl) were resuspended in SDS–PAGE sample buffer (125 mM Tris–HCl, pH 6.8, 5 mM EDTA, 2% β-mercaptoethanol, 5% glycerol, and 2% SDS), incubated for 10 min at 95 °C, subjected to denaturing 12% SDS–PAGE and blotted onto PVDF membrane (Bio-Rad; Hercules, CA). Blocking was done with 0.1% I-Block (Tropix; Bedford, MA). Blots were incubated for 45 min with the detecting antibodies, MAbs 3F4 and 12B2 used at concentrations of 1 μg/ml, or with rabbit polyclonal A7 at a dilution of 1:1000. Subsequently, the membranes were washed with blocking buffer and then reacted with alkaline-phosphatase-conjugated goat anti-mouse IgG (Tropix) at 1:5000 dilution. After final wash, Western-light substrate was applied to the membranes for 5 min. Once the membranes were dry, Kodak films were exposed to the membrane and developed with an X-Omat processor. In some experiments, proteins were digested according to the manufacturer's protocol overnight at 37 °C with endoglycosidaseH and PNGaseF (New England Biolabs, Ipswich, MA) prior to Western blotting.

Immunofluorescence. N2a cells were grown on coverslips in 12-well plates and transiently transfected with the MuPrP encoding plasmid DNA's as described above. Forty-eight hours after transfection the cells were washed once with phosphate-buffered saline (PBS) and fixed with 4% paraformaldehyde for 30 min at room temperature. For permeabilization of the cell membrane, 0.1% Triton X-100 (in PBS) was used after fixation. After washing with PBS, the cells were blocked using a 5% solution of skimmed milk powder for 1 h. Cells were incubated with either 3F4 MAb (2 μg/ml concentration) or A7 rabbit polyclonal antibody (for dual immunofluorescence) at a dilution of 1:200 for 1 h at 4 °C. In the latter experiments, cells were also incubated with a mouse MAb against human giantin, a Golgi apparatus marker (1 μg/ml). Following incubation with the primary antibodies, cells were washed 3–4 times with cold PBS and incubated for 45 min at 4 °C with FITC-conjugated anti-mouse IgG for single immunofluorescence and FITC-conjugated anti-rabbit IgG and Texas-Red-conjugated anti-mouse IgG (Southern Biotech, Birmingham, AL) for colocalization studies. Cells were then washed as before and observed by fluorescence microscopy to determine localization of MuPrP proteins and the Golgi apparatus.

Results

Construction of MuPrP with different combinations of signal sequences

The N- and C-terminal signal sequences of PrP^C play a major role in targeting to the ER, glycosylation and attachment to the cell membrane. Mutations in the N-terminal signal sequence has been shown to increase the proportion of the inverted, transmembrane form of PrP^C and reduce its translocation efficiency [28]. We investigated changes in the *in vitro* tissue culture expression profile of MuPrP resulting from replacement of the wild-type PrP (wt-PrP) N-terminal signal sequence (amino acid residues 1–22) with the signal sequence derived from the human tissue plasminogen activator (tPA, 18 amino acid residues); the resulting plasmid DNA construct was named tPA-PrP. Because the C-terminal GPI anchor attachment signal has been proposed to act as a secondary ER targeting signal, we also constructed wt-PrP-ΔGPI and tPA-PrP-ΔGPI. Comparing the expression patterns among these four constructs should elucidate the roles of both signal peptides in PrP^C trafficking. A final construct, tPA-PrP-ΔC, was constructed to test the effect of a deletion from the central hydrophobic TM domain to the C-terminal GPI anchor attachment domain. As shown in Fig. 1, all of the constructs except tPA-PrP-ΔC retained the complete epitope which is defined by monoclonal antibody (MAb) 3F4.

Expression of different MuPrP constructs in the non-neuronal 293T cells

The expression of modified MuPrP constructs was first examined in transiently transfected non-neuronal human embryonic kidney 293T cells (Fig. 2). The electrophoretic

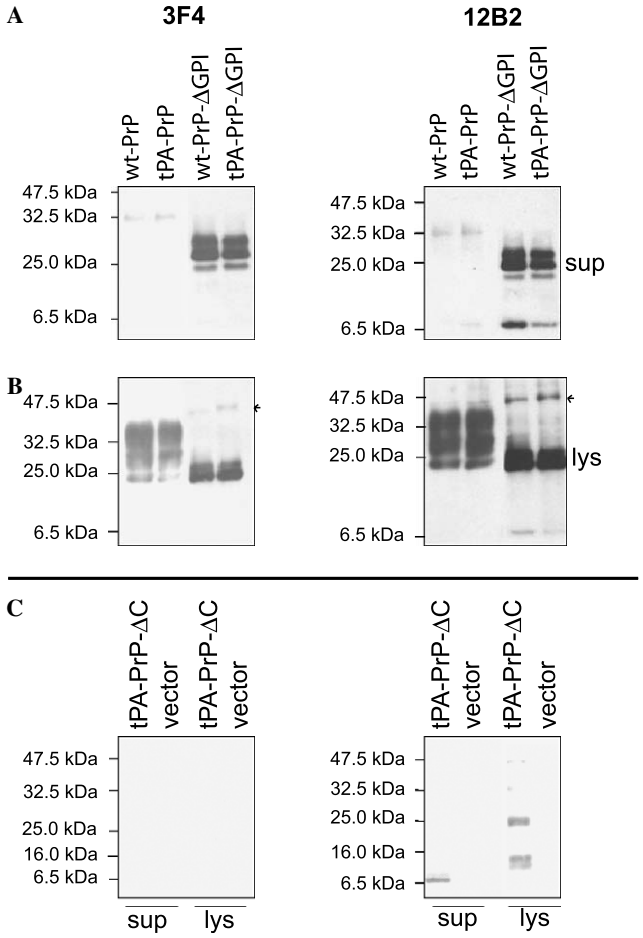

Fig. 2. Expression profile of the different MuPrP constructs in a non-neuronal cell line. Human embryonic kidney 293T cells were transiently transfected with plasmid DNA constructs encoding the full-length and C-terminal GPI anchor attachment signal deleted MuPrP with either the N-terminal wild-type signal sequence or a tPA signal sequence as indicated on top and harvested after 72 h. Immunoblotting of the supernatant (A) and cell lysate (B) fractions were performed. (C) Immunoblotting of the supernatant (sup) and cell lysate (lys) fractions of 293T cells transiently transfected with the MuPrP construct devoid of the entire C-terminal domain including the putative transmembrane domain. Vector DNA lacking any insert was used as a negative control. Immunoblotting was performed with MAbs, 3F4 (left column) and 12B2 (right column). A high molecular weight signal (p46), present in the lysate fraction, is indicated by the arrow.

profiles of the wild-type and modified MuPrP proteins was probed by Western blotting using two prion protein specific MAbs, 12B2 and 3F4. As predicted, both MAbs detected expression of all the PrP constructs except the tPA-PrP-ΔC construct, which was recognized only by 12B2 (Fig. 2C). As expected, supernatant fractions of 293T cells transfected with MuPrP constructs lacking the C-terminal GPI membrane anchor attachment domain (wt-PrP-ΔGPI and tPA-PrP-ΔGPI) contained much higher MuPrP levels than did supernatants from cells expressing the full-length MuPrP constructs (wt-PrP and tPA-PrP) (Fig. 2A). Expression of both wt-PrP and tPA-PrP constructs was readily detected in a cell lysate fraction (Fig. 2B). The levels and patterns of MuPrP expression were not affected by replacing the PrP N-terminal signal sequence with the tPA signal sequence in either the presence or absence of the GPI anchor (Figs. 2A and B).

The intracellular fraction of cells expressing the two full-length MuPrP constructs (wt-PrP and tPA-PrP) contained similar patterns of three distinct groups of bands that corresponded to unglycosylated, monoglycosylated, and diglycosylated PrP species. The unglycosylated species was observed as a single band of 23 kDa, the monoglycosylated species as two juxtaposed bands of molecular weights of 28 and 29 kDa, while the major diglycosylated species migrated as a broad smear in the range of 33–35 kDa (Fig. 2B). Full-length MuPrP was detected in the supernatant fraction as a faint 33 kDa band in wt-PrP and tPA-PrP, indicating that a small fraction of the fully glycosylated MuPrP was secreted. In cells expressing wt-PrP-ΔGPI and tPA-PrP-ΔGPI, both 3F4 and 12B2 detected intracellular expression of a doublet of 21–26 kDa whereas culture supernatants contained three distinct bands, a minor non-glycosylated species at 21 kDa and major glycosylated species at 26 and 28 kDa. These mono- and di-glycosylated species resemble those formed from the full-length prion protein, indicating translocation via the normal secretory pathway in spite of loss of the C-terminal GPI signal sequence, although migration patterns suggest differences in the nature of the attached *N*-glycans. The 12B2 MAb but not the 3F4 MAb detected a low molecular weight signal migrating just above the dye-front in the supernatant fraction of wt-PrP-ΔGPI and tPA-PrP-ΔGPI. A similar signal (~8 kDa) was observed at low level in the intracellular fraction. This is probably an N-terminal product of PrP degradation, as previously described [29]. Interestingly, expression of these GPI anchor-deleted constructs resulted in the appearance of a unique 46 kDa signal (p46) present only in the intracellular fraction. This species was detected more strongly by the 12B2 MAb than the 3F4 antibody in 293T cells (Fig. 2B).

Expression of the tPA-PrP-ΔC construct, which lacks part of the 3F4 epitope, was only detected by 12B2. An 8 kDa band, approximately of the size predicted for the PrP23-110 fragment and similar to the N-terminal fragments in the two ΔGPI constructs, though with slightly higher mobility, was observed in the supernatant fraction. The more complex pattern of intracellular species comprised, in addition to a weak 8 kDa band, a major doublet at 13–14 kDa and a single band at 25 kDa (Fig. 2C). None of the MAbs showed any binding in the supernatant or cell lysate sample from cells transfected with vector DNA lacking a PrP insert (Fig. 2C).

Expression of MuPrP constructs in neuronal cell line N2a

To verify the reproducibility of the appearance of p46, the expression pattern of the MuPrP constructs was re-examined in an entirely different type of cell line, e.g., N2a. Since the expression profiles of both the full-length and

GPI anchor domain-deleted constructs were similar in 293T cells, independent of their N-terminal leader sequences, only the expression of constructs with a tPA leader was examined in transiently transfected neuronal N2a cells. Expression profiles for all PrP constructs were similar to those observed in 293T cells except that 3F4 MAb recognized higher levels of secreted full-length tPA-PrP in the culture medium (Fig. 3A, left panel). Signals recognized by 12B2 MAb were weaker, when compared to the signals observed with 3F4, because of a shorter exposure time. The tPA-PrP construct was still expressed in three glycosylated forms, however, separation of the mono- and diglycosylated species was much less distinct in the intracellular fraction than that observed in 293T cells. Blotting of the cell lysate fraction showed a smear ranging from 28 to 35 kDa with both the MAbs whereas the monoglycosylated species of a 23 kDa band was distinct (Fig. 3B).

The glycosylation status of these species was examined by hydrolysis with either endoglycosidase H or PNGase F prior to sample loading on SDS–PAGE (Fig. 3). In both the supernatant and intracellular fractions, the full-length tPA-PrP products were resistant to endoglycosidase H but sensitive to PNGaseF digestion. The secreted species converted to a single band of 23 kDa upon digestion with PNGaseF, presumably non-glycosylated full-length mature PrP^{C}. In the cell lysate fraction after PNGaseF digestion, 3F4 MAb detected a low molecular weight smear and a distinct band of ~15 kDa in addition to the 23 kDa full-length PrP.

MuPrP protein expressed from the tPA-PrP-ΔGPI construct in lysate of N2a cells was observed as a doublet of two bands migrating very closely to each other at about 24 kDa (Fig. 3B). In the supernatant fraction two major bands at 23 and 26 kDa were observed with a faint band at 28 kDa recognized by MAb 3F4 (Fig. 3A, left panel). As in 293T cells, MAb 12B2 detected a ~8 kDa product in the secreted fraction of N2a cells transfected with this GPI anchor-deleted PrP construct. The secreted tPA-PrP-ΔGPI products were resistant to endoglycosidase H digestion but sensitive to PNGaseF treatment; the two larger molecular weight bands (Fig. 3, left panel) became a single band corresponding to the 21 kDa unglycosylated mature MuPrP species. This change was less obvious for the intracellular products, as the doublet of bands were much closer to each other. Treatment of both the full-length tPA-PrP and the tPA-PrP-ΔGPI protein products with PNGaseF led to appearance of a weak smear of lower molecular weight proteolytic fragment (Fig. 3, left lower panel). Signal corresponding to p46 was also detected in lysates of N2a cells expressing tPA-PrP-ΔGPI, as observed in 293T cell lysates expressing wt-PrP-ΔGPI and tPA-PrP-ΔGPI. PNGaseF mediated deglycosylation of the full-length MuPrP (tPA-PrP) also induced production of a high molecular band that migrated slightly slower than p46. Since no similar high molecular weight signal was observed in the absence of the PNGaseF, we think that p46 is a unique conversion of the unglycosylated PrP species as a result of loss of glycosylation.

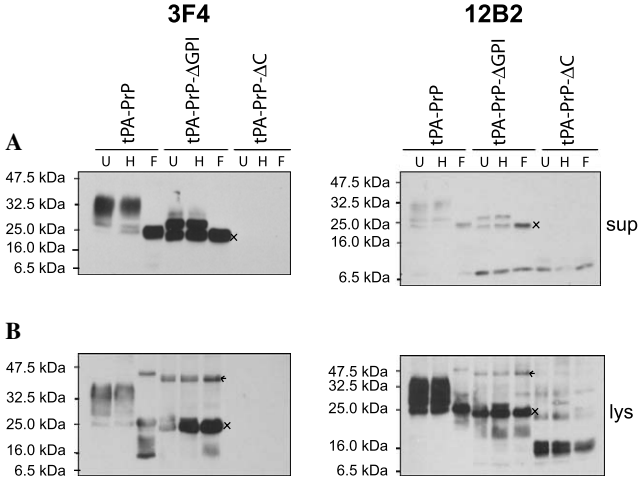

Fig. 3. Expression profile and enzymatic deglycosylation patterns of the different MuPrP constructs in a neuronal cell line, N2a. The constructs, as indicated on top, were transiently transfected in N2a cells which were harvested after 72 h. (A) Cell culture supernatants (sup) and (B) cell lysate (lys) samples from each transfection were either untreated (U) or treated with Endoglycosidase H (H) or PNGase F (F). Immunoblotting was performed with either 3F4 MAb (left column) or 12B2 MAb (right column). A high molecular weight signal (p46), present in the lysate fraction, is indicated by the arrow. Deglycosylated full-length prion protein species (23 kDa) is indicated by a cross.

The expression profile of the tPA-PrP-ΔC construct in N2a cells was identical to that observed in 293T cells. Only the predicted 8 kDa N-terminal fragment was observed in the supernatant fraction, while a predominant doublet at 13–14 kDa was seen in the intracellular fraction. Faint signals corresponding to the 8 kDa N-terminal fragment and other higher molecular weight bands were also observed in the intracellular fraction. None of these expressed products were sensitive to either endoglycosidase H or PNGaseF, indicating that these forms remained unglycosylated, as expected from deletion of the C-terminal domain. Very weak background reactivity to normal N2a cell lysate (untransfected and transfected with vector DNA) was observed for 12B2 indicating detection of endogenous PrP (data not shown).

Effect of inhibition of N-linked glycosylation on the expression of MuPrP constructs

In order to further confirm that deglycosylation of PrP promotes the formation of p46; tPA-PrP and tPA- PrP-ΔGPI constructs were expressed in transiently transfected 293T cells in the presence of tunicamycin to inhibit the N-linked glycosylation. Since O-linked glycosylation of PrP has not been reported, tunicamycin treatment is expected to produce unglycosylated PrP. The intracellular fractions were analyzed on a 12% SDS–PAGE followed by Western blotting with the 12B2 MAb. As expected, the major bands detected in the Western blot were the unglycosylated species. A strong signal corresponding to

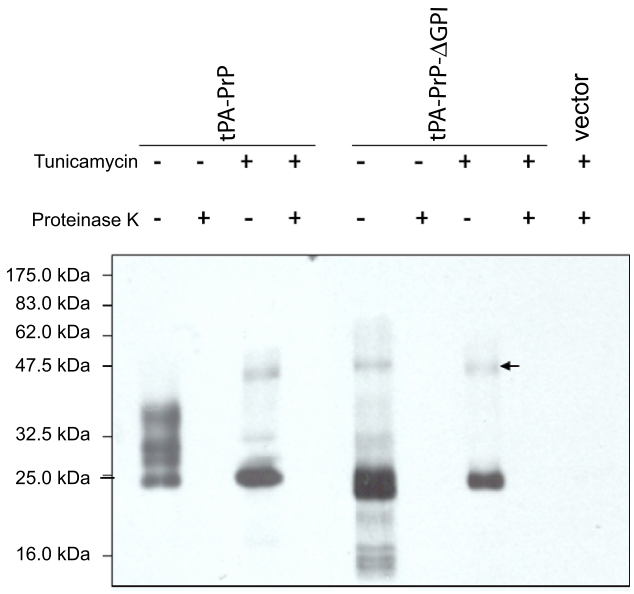

Fig. 4. Inhibition of N-linked glycosylation leads to the formation of p46 which is sensitive to Proteinase K digestion. 293T cells were transiently transfected with plasmid DNA encoding tPA-PrP and tPA-PrP-ΔGPI and transfected cells were maintained for 72 h in the presence of 5 μg/ml tunicamycin. Immunoblotting was performed on the cell lysate using the MAb 12B2. Cell lysate from cells transfected with vector DNA in the presence of tunicamycin was used as a negative control. An aliquot from each sample was digested with Proteinase K (100 μg/ml) to analyze protease sensitivity as indicated on top. A high molecular weight signal (p46) is indicated by the arrow.

that of 46 kDa molecular weight and whose mobility was identical to that observed following transfection with the tPA- PrP-ΔGPI construct (irrespective of treatment with tunicamycin) was observed in the presence of tunicamycin (Fig. 4). Appearance of this unglycosylated dimer reinforces the hypothesis that the previously observed dimerization of MuPrP occurs as a result of loss of *N*-glycosylation. None of the signals including that of p46 were resistant to protease digestion as indicated by complete degradation by digestion with Proteinase K.

Intracellular localization of the MuPrP proteins examined by immunofluorescence and probable nature of p46

Our data indicated that the removal of the GPI anchor sequence led to changes in the MuPrP glycosylation pattern. It also affected the level of MuPrP secretion, implying that early events in the intracellular trafficking of nascent MuPrP are affected by removal of the GPI anchor sequence. Since this should be reflected in the intracellular distribution of MuPrP products, we investigated this distribution in N2a cells transiently transfected with tPA-PrP, tPA-PrP-ΔGPI, and tPA-PrP-ΔC constructs. After N2a cells being transfected for 48 h, indirect immunofluorescence was performed using MAb 3F4 as the primary antibody. When cells were not permeabilized with Triton X-100, cell surface expression of the full-length tPA-PrP was observed (Fig. 5) whereas the surface expression of

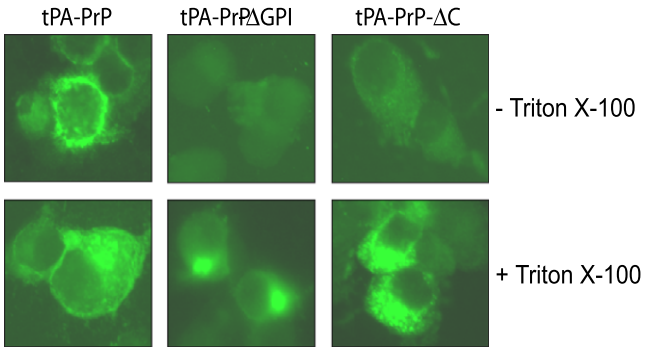

Fig. 5. Cellular localization of full-length MuPrP and its deletion mutants. The indicated plasmid DNA constructs were transiently transfected into N2a cells and immunofluorescence was performed using 3F4 MAb after fixing the cells with 4% paraformaldehyde, with or without permeabilization with Triton X-100, as indicated on the right, to examine cytoplasmic and cell-surface localization respectively, of the relevant prion protein (1000× magnification).

the other two constructs could not be detected. After cells were permeabilized with Triton X-100, expression of tPA-PrP was observed to be scattered in the cytosol. Surprisingly, 3F4 reacted strongly with the intracellularly expressed tPA- PrP-ΔC in its native form, although it failed to detect the denatured protein in Western blots (Fig. 2). Like tPA-PrP, tPA-PrP-ΔC was observed scattered in the cytosol. However, tPA-PrP-ΔGPI was expressed as intense peri-nuclear foci, typical of Golgi localisation. To examine the colocalization of this signal with the Golgi apparatus, dual immunofluorescence was performed including a MAb against giantin, a Golgi marker and a rabbit polyclonal antibody (A7) that has been raised against a dimeric form of MuPrP [24]. As shown in Fig. 6A, in permeabilized N2a cells the localization of tPA- PrP-ΔGPI is confirmed within the Golgi apparatus and is significantly different from the intracellular distribution of full-length tPA-PrP. Immunoblotting of N2a cell-expressed tPA-PrP and tPA-PrP-ΔGPI was performed with A7 and both the supernatant and cell lysate fractions were analyzed (Fig. 6B). Results similar to what were obtained with 3F4 and 12B2 was observed. The p46 was detected in the cell lysate as earlier observations, when MuPrP was expressed devoid of the GPI signal. Additionally a signal of lower molecular weight (~15 kDa) was observed in both the supernatant and the cell lysate fractions. The identity of this protein species which has been observed in the cell lysate fractions earlier (Fig. 3B) is presently unclear.

Discussion

While analyzing the N-linked glycosylation process of MuPrP in a cell culture model, we have shown, for the first time, that when glycosylation of the normal mouse prion protein is prevented or inhibited in tissue culture, a small fraction of the protein converts into a high molecular weight form (p46) which could be detected on a reducing gel. p46 is comprised of MuPrP, recognizable by three different antibodies specific for MuPrP and was found to be

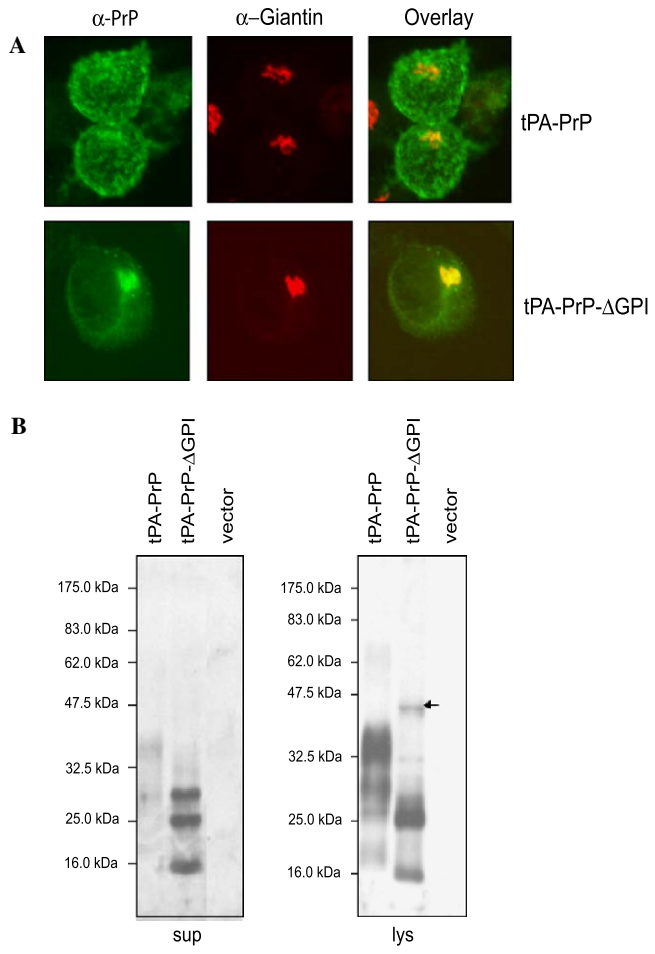

Fig. 6. (A) Colocalization of full-length and GPI anchor signal-deleted MuPrP within the Golgi apparatus. The relevant plasmid DNA construct was used to transiently transfect N2a cells. Dual immunofluorescence was performed in permeabilized cells using A7 rabbit polyclonal antibody raised against dimeric PrP and a mouse MAb against Giantin, a golgi marker. Colocalization was assessed by observing the cells under a fluorescent microscope (1000× magnification). (B) Immunoblotting with a rabbit polyclonal generated against a dimeric MuPrP. N2a cells transiently transfected with tPA-PrP and tPA-PrP-ΔGPI were harvested 72 h post-transfection. The protein profile in the supernatant (sup) and cell lysate (lys) fraction were analyzed by immunoblotting with A7 rabbit polyclonal antibody. The high molecular weight signal (p46), present only in the lysate fraction, is indicated by the arrow.

twice the molecular weight of unglycosylated MuPrP. Additionally, p46 reacted with an antibody generated against a dimeric MuPrP. These evidences lead us to propose that a compromise in the glycosylation machinery of MuPrP in cultured mammalian cells result in the formation of a relatively stable dimer that remains intracellular. The perturbation in the N-linked glycosylation of the prion protein has been studied in several different ways, e.g., removal of the C-terminal GPI anchor attachment signal, enzymatic deglycosylation *in vitro* by treatment with PNGase F, and by protein synthesis in the presence of tunicamycin, a general inhibitor of N-linked glycosylation [30,31]. Previously, the role of the C-terminal GPI anchor in influencing N-linked glycosylation of MuPrP has been assessed by expressing MuPrP in human neuroblastoma SH-SY5Y cells wherein it was found that C-terminal membrane anchorage is required for N-linked glycosylation of MuPrP [32]. The presence of only unglycosylated species of PrP-ΔGPI was reported in both the lysate and the cell culture supernatant. This is in contrast to our observation where we show clearly the presence of glycosylated species of secreted MuPrP in the culture medium (Figs. 2 and 3) which indicates that at least one fraction of the PrP-ΔGPI pool traverses the secretory pathway. Whether this secreted form of PrP-ΔGPI is distinct from the fraction that is localized within the Golgi apparatus (Fig. 6A) remains to be elucidated. Transgenic mice expressing PrP lacking the GPI anchor accumulated extracellular PrP amyloid only when infected with a prion strain of PrP^{Sc}. This abnormal protease-resistant PrP had a considerably reduced N-linked glycosylation pattern [33]. Our observation of a glycosylated form of PrP^{C} devoid of GPI anchor was consistent with an earlier report [29], where mono- and unglycosylated glycoforms of recombinant PrP^{C} were found in the culture medium of DB11 cells stably transfected with MuPrP-ΔGPI. However, neither groups reported observing the presence of p46 MuPrP dimer. Whereas choice of the cell line can be attributed to this cause, we strongly argue against this, as we were able to detect the presence of p46 using two entirely different types of cell lines, a non-neuronal and one of a neuronal origin.

Distinctly different conformations in the p46 dimer are observed when glycosylation loss is achieved in different ways and this argues against the critique that the high molecular weight signal observed in this study results from a non-specific act of protein folding. When loss of glycosylation was achieved by deleting the C -terminal GPI signal or with the presence of an N-linked glycosylation inhibitor, the p46 dimer form of the full-length and the ΔGPI constructs have identical mobility (Fig. 4). However, when MuPrP is enzymatically deglycosylated under cell-free condition, the dimeric form of the full-length protein has a higher mobility than the C-terminal truncated form (Fig. 3). The important question here is whether the formation of p46 dimer and/or its cause, i.e., the glycosylation status of PrP^{C} play a role in causing prion diseases. The hallmark of prion diseases is the change of conformation of the normal cellular prion protein. Our results as well as previous reports indicate that loss of the GPI anchor attachment signal, besides resulting in reduced access to the cellular glycosylation machinery and initiating formation of p46 dimer, also appear to increase susceptibility to proteolysis at the N-terminus, all consistent with a modified PrP conformation. Intracellular accumulation of N-terminally truncated degradation products of glycosylation deficient PrP^{C} has been described before [5]. The destabilization of the prion protein as a result of loss in N-linked glycosylation and apparently combined with additional functions (e.g., membrane attachment function with the help of the TM domain) is clearly manifested with the tPA-PrP-ΔC construct. The theoretical molecular weight

of the amino acid backbone of tPA-PrP-ΔC is approximately 9.8 kDa but the diverse signals that correspond to molecular weights from 25 to 8 kDa indicate that this protein has a complex trafficking after its biosynthesis. After its translocation in the lumen of the ER, unlike the full-length and ΔGPI proteins it is probably not integrated in the membrane and is misfolded. This misfolded protein remains unutilized by the enzymes in the glycosylation pathway resulting in probable destabilization and accumulation of the protein in several conformations. Replacement of the wild-type N-terminal signal sequence, a major player in directing a nascent protein through the post-translational processing pathway, with a heterologous signal peptide did not alter the overall glycosylation status of MuPrP.

A role for prion dimerization in scrapie replication was suggested as early as 1979 by Dickinson and Outram [34]. Although PrP^{C} is usually described as a monomer, various reports have described dimeric forms of both PrP^{C} and the scrapie-associated prion protein [35–40]. Dimerization, however, has not been associated with N-linked glycosylation or any other modifications in post-translational processing of the prion protein. On the other hand, biophysical studies have delineated the role of the dimeric form of either PrP^{C} or PrP^{Sc} in the conformational transition to fibril formation [34,41]. While infectious PrP^{Sc} is apparently a soluble oligomeric precursor of the amyloid form that can directly recruit PrP^{C} to its termini [42], the stochastic process of sporadic PrP^{Sc} formation must start with monomer–dimer interconversion. Conversion from a monomeric to a dimeric form may require additional factors such as molecular chaperones, protein-X [43] or disulphide rearrangement [34] and may also be promoted by deglycosylation as demonstrated in this study. A relatively stable non-glycosylated cytoplasmic dimer, produced as a result of defective trafficking or N-linked glycosylation, therefore, is a plausible intermediate for a role in sporadic or spontaneous conversion to the infectious oligomer. Stabilization of these dimers through hairpin stacking of β-sheets, requiring a large scale rearrangement of the α-helical domains, would facilitate conversion to a PrP^{C} oligomer. Further high affinity interactions of dimers and oligomers may induce formation of amyloid fibrils and these interactions may also be influenced by mutation, pH and membrane proximity [41]. Thus, while the p46 dimer which we have observed was Proteinase K sensitive (Fig. 4), its formation may be one of the earliest steps toward the structural alteration of PrP^{C} required for conversion to PrP^{Sc}.

The intracellular localization of this dimer (Fig. 6A) also reinforce the conclusion made by a recent observation where visualization of prion infection in transgenic mice expressing GFP-tagged PrP^{C} [44], suggested that production of PrP^{Sc} from PrP^{C} occurred in the Golgi apparatus. Our immunofluorescence studies showed that the wt-PrP-ΔGPI and tPA-PrP-ΔGPI constructs used in this study do not reach the cell surface. These proteins have two major destinations. One fraction remains mostly unglycosylated with low level expression of apparently monoglycosylated forms and is found only in the intracellular fraction, retained within the Golgi apparatus, as shown by dual immunofluorescence studies with giantin, while the other fraction as described earlier follows the secretory pathway. The dimeric MuPrP formed under these conditions was found to be restricted within this intracellular fraction as cross identified by the A7 polyclonal antibody that was raised against a dimeric form of MuPrP (Fig. 6). The argument that the expression levels of the dimeric form of glycosylation deficient MuPrP elsewhere in the cytosol is below the detection limits of the assay can be countered by the fact that undetectable tPA-PrP-ΔC construct on the Western blot by 3F4 could be detected by our immunofluorescence assay. Future direction in this project would be directed towards the kinetics of the formation of p46, its characterization and purification and to show its association with disease forms of the prion protein.

Acknowledgments

We thank Dr. D.A. Harris, Washington University, St. Louis, MO for the plasmid DNA encoding the full-length MuPrP with the 3F4 tag, Dr. Vishwanath Lingappa University of California, San Francisco, for 3F4 Mab, Dr. H.M. Schatzl, Technical University of Munich, Munich, Germany for A7 rabbit polyclonal serum. The MAb against the Golgi apparatus marker giantin was a gift from Dr. H.P. Hauri, University of Basel, Switzerland. Production of MAb 12B2 was funded by the Dutch Ministry of Agriculture, Environmental Management and Food (8041869000), and epitope mapping by NeuroPrion STOPPrions (FOOD-CT-2004-506579). Karel Riepema, Esther de Jong, and Jorg Jacobs are acknowledged for skillful generation and characterization of antibody 12B2. Part of the research is partially supported by the NIH/NIAID Grant U01 AI 056536. The authors would like to thank Dr. Te-hui W. Chou for her critical comments.

References

[1] S.B. Prusiner, Prion diseases and the BSE crisis, Science 278 (1997) 245–251.
[2] S.B. Prusiner, Novel proteinaceous infectious particles cause scrapie, Science 216 (1982) 136–144.
[3] K. Basler, B. Oesch, M. Scott, D. Westaway, M. Walchli, D.F. Groth, M.P. McKinley, S.B. Prusiner, C. Weissmann, Scrapie and cellular PrP isoforms are encoded by the same chromosomal gene, Cell 46 (1986) 417–428.
[4] V.A. Lawson, S.J. Collins, C.L. Masters, A.F. Hill, Prion protein glycosylation, J. Neurochem. 93 (2005) 793–801.
[5] M. Rogers, A. Taraboulos, M. Scott, D. Groth, S.B. Prusiner, Intracellular accumulation of the cellular prion protein after mutagenesis of its Asn-linked glycosylation sites, Glycobiology 1 (1990) 101–109.
[6] S. Lehmann, D.A. Harris, Blockade of glycosylation promotes acquisition of scrapie-like properties by the prion protein in cultured cells, J. Biol. Chem. 272 (1997) 21479–21487.
[7] S.J. DeArmond, H. Sanchez, F. Yehiely, Y. Qiu, A. Ninchak-Casey, V. Daggett, A.P. Camerino, J. Cayetano, M. Rogers, D. Groth, M.

Torchia, P. Tremblay, M.R. Scott, F.E. Cohen, S.B. Prusiner, Selective neuronal targeting in prion disease, Neuron 19 (1997) 1337–1348.
[8] E. Grasbon-Frodl, H. Lorenz, U. Mann, R.M. Nitsch, O. Windl, H.A. Kretzschmar, Loss of glycosylation associated with the T183A mutation in human prion disease, Acta Neuropathol. (Berlin) 108 (2004) 476–484.
[9] R. Nitrini, S. Rosemberg, M.R. Passos-Bueno, L.S. da Silva, P. Iughetti, M. Papadopoulos, P.M. Carrilho, P. Caramelli, S. Albrecht, M. Zatz, A. LeBlanc, Familial spongiform encephalopathy associated with a novel prion protein gene mutation, Ann. Neurol. 42 (1997) 138–146.
[10] N. Stahl, D.R. Borchelt, K. Hsiao, S.B. Prusiner, Scrapie prion protein contains a phosphatidylinositol glycolipid, Cell 51 (1987) 229–240.
[11] D.A. Harris, Trafficking, turnover and membrane topology of PrP, Br. Med. Bull. 66 (2003) 71–85.
[12] S.L. Shyng, M.T. Huber, D.A. Harris, A prion protein cycles between the cell surface and an endocytic compartment in cultured neuroblastoma cells, J. Biol. Chem. 268 (1993) 15922–15928.
[13] E.T. Parkin, N.T. Watt, A.J. Turner, N.M. Hooper, Dual mechanisms for shedding of the cellular prion protein, J. Biol. Chem. 279 (2004) 11170–11178.
[14] C.D. Lopez, C.S. Yost, S.B. Prusiner, R.M. Myers, V.R. Lingappa, Unusual topogenic sequence directs prion protein biogenesis, Science 248 (1990) 226–229.
[15] F. Perini, R. Vidal, B. Ghetti, F. Tagliavini, B. Frangione, F. Prelli, PrP27-30 is a normal soluble prion protein fragment released by human platelets, Biochem. Biophys. Res. Commun. 223 (1996) 572–577.
[16] P. Parizek, C. Roeckl, J. Weber, E. Flechsig, A. Aguzzi, A.J. Raeber, Similar turnover and shedding of the cellular prion protein in primary lymphoid and neuronal cells, J. Biol. Chem. 276 (2001) 44627–44632.
[17] S.G. Chen, D.B. Teplow, P. Parchi, J.K. Teller, P. Gambetti, L. Autilio-Gambetti, Truncated forms of the human prion protein in normal brain and in prion diseases, J. Biol. Chem. 270 (1995) 19173–19180.
[18] J.F. Richmond, S. Lu, J.C. Santoro, J. Weng, S.L. Hu, D.C. Montefiori, H.L. Robinson, Studies of the neutralizing activity and avidity of anti-human immunodeficiency virus type 1 Env antibody elicited by DNA priming and protein boosting, J. Virol. 72 (1998) 9092–9100.
[19] R.J. Kascsak, R. Rubenstein, P.A. Merz, M. Tonna-DeMasi, R. Fersko, R.I. Carp, H.M. Wisniewski, H. Diringer, Mouse polyclonal and monoclonal antibody to scrapie-associated fibril proteins, J. Virol. 61 (1987) 3688–3693.
[20] H. Bueler, M. Fischer, Y. Lang, H. Bluethmann, H.P. Lipp, S.J. DeArmond, S.B. Prusiner, M. Aguet, C. Weissmann, Normal development and behaviour of mice lacking the neuronal cell-surface PrP protein, Nature 356 (1992) 577–582.
[21] L.J. van Keulen, B.E. Schreuder, R.H. Meloen, M. Poelen-van den Berg, G. Mooij-Harkes, M.E. Vromans, J.P. Langeveld, Immunohistochemical detection and localization of prion protein in brain tissue of sheep with natural scrapie, Vet. Pathol. 32 (1995) 299–308.
[22] G.J. Garssen, L.J. Van Keulen, C.F. Farquhar, M.A. Smits, J.G. Jacobs, A. Bossers, R.H. Meloen, J.P. Langeveld, Applicability of three anti-PrP peptide sera including staining of tonsils and brainstem of sheep with scrapie, Microsc. Res. Tech. 50 (2000) 32–39.
[23] C.M. Thuring, J.H. Erkens, J.G. Jacobs, A. Bossers, L.J. Van Keulen, G.J. Garssen, F.G. Van Zijderveld, S.J. Ryder, M.H. Groschup, T. Sweeney, J.P. Langeveld, Discrimination between scrapie and bovine spongiform encephalopathy in sheep by molecular size, immunoreactivity, and glycoprofile of prion protein, J. Clin. Microbiol. 42 (2004) 972–980.
[24] S. Gilch, F. Wopfner, I. Renner-Muller, E. Kremmer, C. Bauer, E. Wolf, G. Brem, M.H. Groschup, H.M. Schatzl, Polyclonal anti-PrP auto-antibodies induced with dimeric PrP interfere efficiently with PrPSc propagation in prion-infected cells, J. Biol. Chem. 278 (2003) 18524–18531.
[25] A. Schweizer, J.A. Fransen, T. Bachi, L. Ginsel, H.P. Hauri, Identification, by a monoclonal antibody, of a 53-kDa protein associated with a tubulo-vesicular compartment at the *cis*-side of the Golgi apparatus, J. Cell Biol. 107 (1988) 1643–1653.
[26] P. Leblanc, D. Baas, J.L. Darlix, Analysis of the interactions between HIV-1 and the cellular prion protein in a human cell line, J. Mol. Biol. 337 (2004) 1035–1051.
[27] S. Wang, D. Heilman, F. Liu, T. Giehl, S. Joshi, X. Huang, T.H. Chou, J. Goguen, S. Lu, A DNA vaccine producing LcrV antigen in oligomers is effective in protecting mice from lethal mucosal challenge of plague, Vaccine 22 (2004) 3348–3357.
[28] R.S. Stewart, D.A. Harris, Mutational analysis of topological determinants in prion protein (PrP) and measurement of transmembrane and cytosolic PrP during prion infection, J. Biol. Chem. 278 (2003) 45960–45968.
[29] D.B. Brimacombe, A.D. Bennett, F.S. Wusteman, A.C. Gill, J.C. Dann, C.J. Bostock, Characterization and polyanion-binding properties of purified recombinant prion protein, Biochem. J. 342 (Pt. 3) (1999) 605–613.
[30] L. Lehle, W. Tanner, The specific site of tunicamycin inhibition in the formation of dolichol-bound *N*-acetylglucosamine derivatives, FEBS Lett. 72 (1976) 167–170.
[31] D.K. Struck, W.J. Lennarz, Evidence for the participation of saccharide-lipids in the synthesis of the oligosaccharide chain of ovalbumin, J. Biol. Chem. 252 (1977) 1007–1013.
[32] A.R. Walmsley, F. Zeng, N.M. Hooper, Membrane topology influences *N*-glycosylation of the prion protein, EMBO J. 20 (2001) 703–712.
[33] B. Chesebro, M. Trifilo, R. Race, K. Meade-White, C. Teng, R. LaCasse, L. Raymond, C. Favara, G. Baron, S. Priola, B. Caughey, E. Masliah, M. Oldstone, Anchorless prion protein results in infectious amyloid disease without clinical scrapie, Science 308 (2005) 1435–1439.
[34] P. Tompa, G.E. Tusnady, P. Friedrich, I. Simon, The role of dimerization in prion replication, Biophys. J. 82 (2002) 1711–1718.
[35] C.G. Bellinger-Kawahara, E. Kempner, D. Groth, R. Gabizon, S.B. Prusiner, Scrapie prion liposomes and rods exhibit target sizes of 55,000 Da, Virology 164 (1988) 537–541.
[36] P.E. Bendheim, D.C. Bolton, A 54-kDa normal cellular protein may be the precursor of the scrapie agent protease-resistant protein, Proc. Natl. Acad. Sci. USA 83 (1986) 2214–2218.
[37] K.J. Knaus, M. Morillas, W. Swietnicki, M. Malone, W.K. Surewicz, V.C. Yee, Crystal structure of the human prion protein reveals a mechanism for oligomerization, Nat. Struct. Biol. 8 (2001) 770–774.
[38] R.K. Meyer, A. Lustig, B. Oesch, R. Fatzer, A. Zurbriggen, M. Vandevelde, A monomer–dimer equilibrium of a cellular prion protein (PrPC) not observed with recombinant PrP, J. Biol. Chem. 275 (2000) 38081–38087.
[39] S.A. Priola, B. Caughey, K. Wehrly, B. Chesebro, A 60-kDa prion protein (PrP) with properties of both the normal and scrapie-associated forms of PrP, J. Biol. Chem. 270 (1995) 3299–3305.
[40] T.K. Sklaviadis, L. Manuelidis, E.E. Manuelidis, Physical properties of the Creutzfeldt–Jakob disease agent, J. Virol. 63 (1989) 1212–1222.
[41] J. Warwicker, Modeling a prion protein dimer: predictions for fibril formation, Biochem. Biophys. Res. Commun. 278 (2000) 646–652.
[42] D.A. Kocisko, J.H. Come, S.A. Priola, B. Chesebro, G.J. Raymond, P.T. Lansbury, B. Caughey, Cell-free formation of protease-resistant prion protein, Nature 370 (1994) 471–474.
[43] K. Kaneko, L. Zulianello, M. Scott, C.M. Cooper, A.C. Wallace, T.L. James, F.E. Cohen, S.B. Prusiner, Evidence for protein X binding to a discontinuous epitope on the cellular prion protein during scrapie prion propagation, Proc. Natl. Acad. Sci. USA 94 (1997) 10069–10074.
[44] S.J. Barmada, D.A. Harris, Visualization of prion infection in transgenic mice expressing green fluorescent protein-tagged prion protein, J. Neurosci. 25 (2005) 5824–5832.